Numerical estimates of the generalized dimensions of the Hénon attractor for negative *q*

1996 J. Phys. A: Math. Gen. 29 L391

(http://iopscience.iop.org/0305-4470/29/15/005)

J. Phys. A: Math. Gen. **29** (1996) L391–L398. Printed in the UK

LETTER TO THE EDITOR

Numerical estimates of the generalized dimensions of the Hénon attractor for negative q

Romualdo Pastor-Satorras†‡¶ and Rudolf H Riedi§+

† Departament de Física Fonamental, Facultat de Física, Universitat de Barcelona, Diagonal 647, E-08028 Barcelona, Spain

‡ Centre d'Estudis de la Complexitat, Museu de la Ciència de la Fundació 'la Caixa', Teodor Roviralta 55, E-08022 Barcelona, Spain

§ Yale University, Mathematics Department, 10 Hillhouse Ave, New Haven, CT 06520-8283, USA

Received 12 February 1996, in final form 29 May 1996

Abstract. The usual fixed-size box-counting algorithms are inefficient for computing generalized fractal dimensions in the range of $q < 0$. In this letter we describe a new numerical algorithm specifically devised to estimate generalized dimensions for large negative q, providing evidence of its better performance. We compute the complete spectrum of the Hénon attractor, and interpret our results in terms of a 'phase transition' between different multiplicative laws.

Much effort has been devoted in recent years to the study of the fractal patterns [1] exhibited by many physical systems such as diffusion-limited aggregation [2], viscous fingering [3] and chaotic attractors of nonlinear dynamical systems [4]. It has become clear, however, that many natural fractal objects are actually *multifractals* [5, 6], that is, they are composed of an infinite set of interwoven subfractals, characterized by a *multifractal spectrum* $f(\alpha)$ (see [7–10] and references therein). The usual fixed-size box-counting multifractal formalism for a general measure μ on $\mathbb{R}^d$ considers the so-called *partition sum* $Z_\varepsilon(q) = \sum_{\mu(B)\neq 0}(\mu(B))^q$, $q \in \mathbb{R}$, where the sum runs over all boxes B of side ε taken from an ε-grid G_ε, i.e.

$$B = \prod_{k=1}^{d}[l_k\varepsilon, (l_k+1)\varepsilon[\tag{1}$$

l_k being integer numbers. The *generalized dimensions* D_q [9–12] are then mathematically defined by the limit

$$D_q = \frac{1}{q-1}\lim_{\varepsilon\to 0}\frac{\log Z_\varepsilon(q)}{\log\varepsilon}. \tag{2}$$

The $f(\alpha)$ spectrum is then given by the Legendre transformation $f(\alpha) = \min_\alpha\{q\alpha - (q-1)D_q\}$ [7–10].

These definitions, though temptingly simple and rigorous, cause problems even in their pure mathematical application. To be more precise, it can be shown that the limit (2), if it exists, can only be ∞ for $q < 0$ [9]. This is obviously due to the presence of boxes B with an unnaturally small measure, which contribute to the function Z with a diverging term. Serious problems also arise when translating this mathematical notion into a numerical

¶ E-mail address: romu@hermes.ffn.ub.es

+ E-mail address: riedi@math.yale.edu

algorithm, which we will call the *standard algorithm* (SA) in the following. This algorithm computes an estimate $D(q)$ of the mathematical dimension D_q as the slope of a least-squares fitting of $\log(Z_\varepsilon(q))/(q-1)$ against $\log(\varepsilon)$. The SA proves to be slowly convergent and it works well only for $q > 1$ and only for measures in $\mathbb{R}^d$ with $d \leqslant 2$, being especially problematic in the region $q < 0$ [13, 14]. Some attempts have been made in order to design efficient fixed-size box-counting algorithms [15–17], but all of them fail when dealing with negative q.

In a recent paper [9] one of the authors proposed a new mathematical multifractal formalism, devised to overcome the drawbacks for negative q. The basic idea is very simple: if we do not assume *a priori* knowledge on the distribution μ, we cannot prevent, given an arbitrary ε-grid, some boxes B meeting μ only in a very small part. Such a box B possesses an extremely small and unnatural measure and, hence, constitutes a very poor approximation of a ball centred in a point on the distribution. For large positive q, such mismatching boxes can be neglected since their contribution to Z is almost null. But this is not true for negative q.

From an intuitive point of view, a naive way to cure this problem is to consider the measure of *extended boxes* B^*, obtained by expanding a given box $B \in G_\varepsilon$ by a factor 3, i.e. (with reference to equation (1))

$$B^* = \prod_{k=1}^{d} [(l_k - 1)\varepsilon, (l_k + 1 + 1)\varepsilon[.$$

Using the *extended partition sum* Z^* [9]

$$Z_\varepsilon^*(q) = \sum_{\mu(B)\neq 0} (\mu(B^*))^q, \tag{3}$$

we formally define the *extended generalized dimensions* D_q^* as

$$D_q^* = \frac{1}{q-1} \lim_{\varepsilon\to 0} \frac{\log Z_\varepsilon^*(q)}{\log \varepsilon}. \tag{4}$$

From a theoretical point of view, D_q^* performs much better than D_q. It can be proven [9] that the limit (4) is the same if the continuous ε is restricted to any sequence ε_n with $\varepsilon_{n+1} \geqslant \nu\varepsilon_n$ for some $1 > \nu > 0$. In addition, D_q^* is invariant under *bilipschitz* coordinate transformations, it coincides with D_q as defined in (2) for $q \geqslant 0$ and produces the expected, meaningful results for self-similar measures.

In this letter we describe a numerical algorithm implementing this new multifractal formalism, which we will call in the following the *enlarged box algorithm* (EBA). The application of the EBA will allow us to determine, for the first time, a fixed-size box-counting estimate of the complete multifractal spectrum of the Hénon attractor [18] (that is, both positive and negative q).

We consider distributions μ as being approximated by a sample of N discrete points from the attractor of some dynamical system. Given an ε-grid of boxes of side ε, the occupation number $n_i(\varepsilon)$ of the ith box is defined as the number of sample points it contains. The natural measure μ_i of box B_i is defined by the fraction of time which a generic trajectory on the attractor spends in that box [12], and is roughly equal to $n_i(\varepsilon)/N$ in the limit of large N. The implementation of SA thus estimates the generalized dimension $D(q)$ as the slope of a linear fit of

$$\frac{1}{q-1} \log Z_\varepsilon(q) \sim \frac{1}{q-1} \log \left(\sum_i (n_i(\varepsilon))^q \right) \tag{5}$$

against $\log \varepsilon$. Note that we have dropped the normalization factor $N = \sum_i n_i(\varepsilon)$ since it is independent of ε. To implement EBA, we replace the occupation numbers $n_i(\varepsilon)$ by the *extended occupation numbers* $n_i^*(\varepsilon)$ which are defined by

$$n_i^*(\varepsilon) = \sum_{j:\, B_j \subseteq B_i^*} n_j(\varepsilon)$$

that is, the number of sample points contained in the box B_i and in all its $3^d - 1$ neighbouring boxes. The implementation of EBA thus computes an estimate $D^*(q)$ of D_q^* as the slope of a linear fit of

$$\frac{1}{q-1} \log Z_\varepsilon^*(q) \sim \frac{1}{q-1} \log \left(\sum_i (n_i^*(\varepsilon))^q \right) \tag{6}$$

against $\log \varepsilon$. As with the SA, we do not include a normalization term $N^*(\varepsilon) = \sum_i n_i^*$. From a strictly mathematical point of view, and due to the limit $\varepsilon \to 0$ in (4), the normalization plays no role, since even though $N^*(\varepsilon)$ is not constant, it is bounded: $N \leqslant N^*(\varepsilon) \leqslant 3^d N$. From a numerical point of view, we experimentally find that definition (6) works well for the measures we investigated. Moreover, the inclusion of the normalization factor results in poorer correlation coefficients and larger error bars. We thus infer that, when performing the linear regression in a range of sufficiently small values of ε, we can neglect the effects of normalization. Unfortunately, as $N^*(\varepsilon)$ is not constant, the convergence is affected by this procedure in the neighbourhood of $q = 1$. Consequently, the estimate of D_1 provided by EBA should be taken with care.

Table 1. Comparison of some numerical values from the SA and EBA with the analytic result D_q for a deterministic fixed-size measure.

Analytical result	SA	EBA
$D_{40} = 1.0256$	$D(40) = 1.02$	$D^*(40) = 1.02$
$D_{10} = 1.1097$	$D(10) = 1.11$	$D^*(10) = 1.11$
$D_0 = 1.5850$	$D(0) = 1.62$	$D^*(0) = 1.62$
$D_{-5} = 2.0322$	—	$D^*(-5) = 1.99$
$D_{-10} = 2.1963$	—	$D^*(-10) = 2.17$
$D_{-25} = 2.3222$	—	$D^*(-25) = 2.30$
$D_{-50} = 2.3677$	—	$D^*(-50) = 2.34$

In order to check the accuracy of our algorithm, we have applied both the SA and the EBA to some self-similar deterministic multifractal measures on $\mathbb{R}^2$ [8–10] constructed with the 'Chaos Game' [19]. Among others, we considered a *fixed-size* measure with contraction factor $r = 1/2$ and probabilities $p_1 = 3/16$, $p_2 = 5/16$, and $p_3 = 8/16$; and a *fixed-mass* measure, with $r_1 = 0.6$, $r_2 = 0.4$, and $r_3 = 0.3$, and probabilities $p = 1/3$. To allow for comparison, we have chosen the parameters exactly as in [20] where both measures are solved analytically. Figures 1(a) and (b) depict the analytical dimension D_q, together with the estimates from the SA and EBA, for the fixed-size and fixed-mass measures, respectively. Table 1 also provides some numerical values for the first measure. For the computations we have averaged 50 different approximations of the measures, each one composed by $N = 50\,000$ points. Linear regressions were performed over an interval of 1.5 decades. Statistical errors from the regression algorithm yield error bars of about 0.01, except for SA at negative q. From our data we conclude that both the SA and the EBA provide fairly good estimates for $q \geqslant -2$. The EBA, however, shows better regression coefficients and slightly smaller error bars. For $q < -2$, the SA suffers from unacceptable regression coefficients and its output is, as expected, meaningless. On the other hand, the estimates of the generalized dimensions from EBA are in excellent agreement with the analytical values over the whole range of negative q analysed (compare table 1).

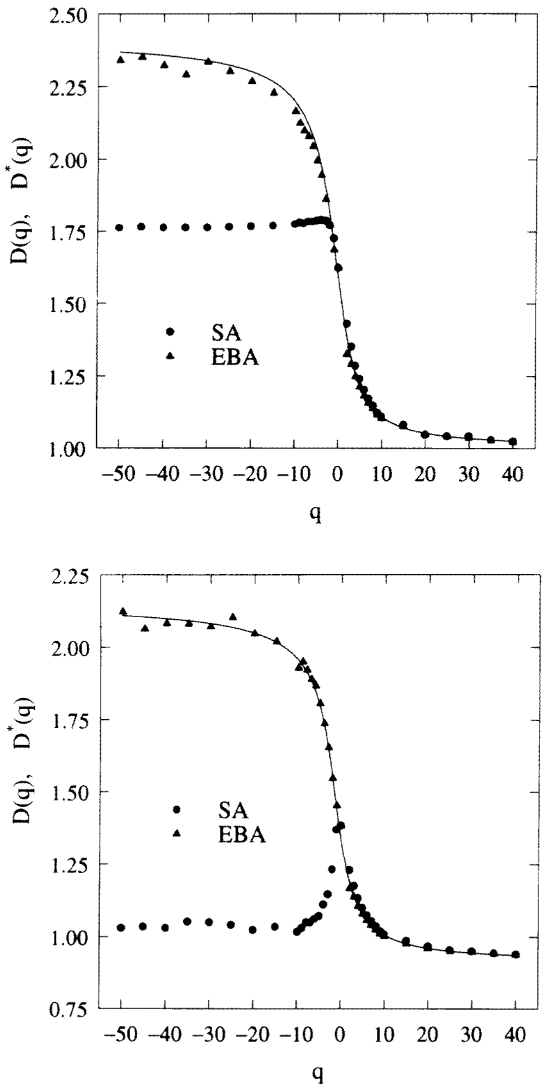

Figure 1. (a) Generalized dimensions from the SA and EBA for a deterministic fixed-size measure. (b) The same for a deterministic fixed-mass measure. The full curves in both figures correspond to the analytical value D_q [20].

Finally, we considered the standard Hénon attractor [18], with parameters $a = 1.4$ and $b = 0.3$. We analysed averages over 50 different realizations of the attractor, each one composed of $N = 150\,000$ points. Linear regressions were performed over an interval between $\varepsilon_{\min} = 10^{-2.5}$ and $\varepsilon_{\max} = 10^{-1}$. Figure 2 shows the scaling region of the (unnormalized) extended partition sum Z^* for different values of q. The linear fits are

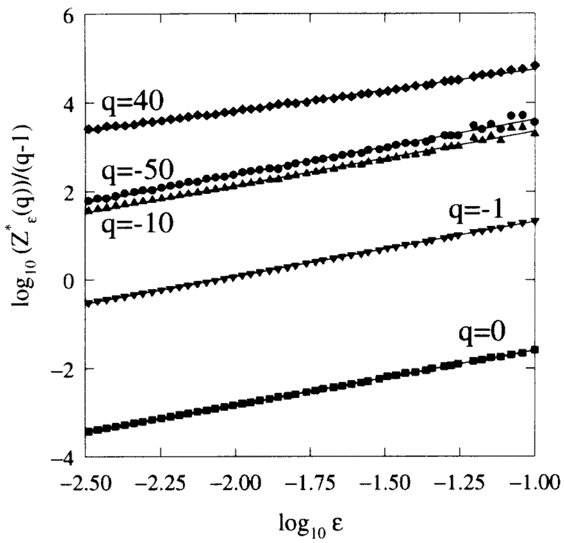

Figure 2. Log–log plot of the unnormalized extended partition sum Z^* of the natural measure on the Hénon attractor as a function of ε, for different values of q.

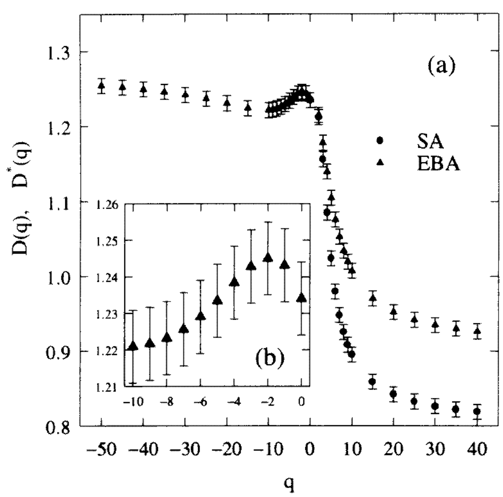

Figure 3. (a) Generalized dimensions from the SA and EBA for the natural measure on the Hénon attractor. Being meaningless, the values of the SA for $q < 0$ have not been plotted. (b) Detail of the region $-10 \leqslant q \leqslant 0$.

excellent, even for a negative value as large as $q = -50$. In figure 3 we have plotted the estimates from the SA and the EBA; table 2 shows some numerical values, together with theoretical predictions and other numerical estimates from box-counting algorithms. The results shown in figure 3 present several remarkable features that deserve some discussion:

(i) In the region of positive q we have found that $D^*(q) > D(q)$. The values estimated with the SA are similar to those found by other authors by means of fixed-size [21] and fixed-mass [22] box-counting algorithms. On the other hand, the results from the EBA are

Table 2. Hénon attractor: Comparison of the performance of the SA and EBA with both theoretical predictions and other numerical estimates.

Theoretical predictions	Numerical estimates	SA	EBA
$D_{-\infty} = 1.352$[a]	$D(-\infty) \simeq 1.5$[b]	—	$D^*(-50) = 1.26$
$D_{-6} \simeq 1.3$[c]	—	—	$D^*(-6) = 1.23$
$D_0 = 1.276$[d]	$D(0) = 1.259$[e]	$D(0) = 1.23$	$D^*(0) = 1.23$
—	$D(2) = 1.199$[e]	$D(2) = 1.21$	$D^*(2) = 1.21$
$D_6 \simeq 1.05$[c]	—	$D(6) = 0.98$	$D^*(6) = 1.08$
—	$D(40) \simeq 0.8$[f]	$D(40) = 0.82$	$D^*(40) = 0.93$
$D_\infty \leqslant 0.84$[g]	$D(\infty) \simeq 0.87$[b]		

[a] [24].
[b] [22], estimate from figure 2.
[c] [23], estimate from figure 1.
[d] [23].
[e] [21].
[f] [21], estimate from figure 2.
[g] [13].

somewhat larger, out of the error bars. They are, however, in close agreement with some theoretical predictions, as shown in table 2. It is known that the generalized dimensions of chaotic attractors computed from standard box-counting algorithms are significantly below the theoretical predictions. This fact is considered to be a fundamental limitation of this sort of algorithm [21], and it is attributed to the local properties of the natural measure in those sets. The measure is extremely inhomogeneous in some regions, which produces a non-convergence of the partition sum and hence an oscillating behaviour by the regression lines used to estimate $D(q)$. Table 2 shows that the EBA is, in some cases, closest to the theoretical predictions, especially for the extended Kaplan–Yorke relation approach in [23]. This better performance of the EBA could be connected with the smoothing effect of the extended boxes, which would attenuate the inhomogeneities of the measure. We would like to note, however, the disagreement with the prediction $D_\infty \leqslant 0.84$ from [13].

(ii) As far as we are aware, we have computed, for the first time, a fixed-size box-counting estimate of $D_{-\infty}$ for the Hénon attractor (around 1.3). This value is in very good agreement with theoretical predictions in which $D_{-\infty}$ is conjectured to be 1.352 [24]. We would like to stress, however, the disagreement with the fixed-mass estimate around 1.5 in [22].

(iii) $D^*(q)$ shows a striking inflection in the region $-10 < q < 0$ (see figure 3(b) for a detail). This inflection is larger than the error bars (around 0.01) so that it does not seem to be ascribable to a mere statistical fluctuation in our results. Moreover, the inflection turns out to be very robust: it does not disappear when shifting the limits of the linear fit, increasing the number of sample points N or the number of boxes in the discretization of ε, or even when normalizing the extended partition sum Z^*_ε. This latter fact excludes a possible malfunctioning of the EBA due to the omission of the normalization factor $N^*(\varepsilon)$ (compare the earlier discussion of equation (6)). Since the D_q spectra are known to monotonically decrease with growing q [12], we view the mentioned inflection as a numerical consequence of the very property of the Hénon attractor's measure which we interpret as a 'phase transition' between the multiplicative laws ruling the different regions of the attractor. Dense regions dominate the behaviour of D_q for $q \gg 0$, while sparse regions prevail for $q \ll 0$. Given that the Hénon attractor is not self-similar [13], it could be possible that the measure would show very different multiplicative laws in each of these regions. In the limiting cases $|q| \gg 1$ we would observe a dominant behaviour and a well defined function D_q^*; therefore, we would then obtain an accurate estimation $D^*(q)$. In the intermediate range $q \sim 0$ ($q < 0$), however, both multiplicative behaviours would be seen at the same time and the inflection would then appear as a numerical artifact of the algorithm, related to the prefactor in the asymptotic power law $Z_\varepsilon^*(q) \sim \varepsilon^{(q-1)D^*(q)}$. For self-similar measures this prefactor $a = \lim_{\varepsilon\to 0} Z_\varepsilon^*(q)\varepsilon^{-(q-1)D^*(q)}$ can be computed and shown to exist by a simple application of the well known renewal theorem [25]). In fact, it follows that a depends heavily on the parameters of the multiplicative process producing the self-similar measure. The prefactor has, therefore, considerable influence on the value of $D^*(q)$ estimated by a linear regression, thus giving rise to a larger indeterminacy which would account for the observed inflection. To support this point of view we would like to mention two related phenomena. First, with superpositions of two self-similar measures we observe numerical behaviour of a similar kind, which are not found in the spectrum D_q defined through a mathematical limit [26]. Second, we note that there are self-affine measures with non-differentiable spectrum D_q^* [27]. The irregular points on the spectrum naturally cause similar numerical problems. They correspond, as is shown in [27], to one eigendirection gaining or losing influence on the partition sum Z^* as q varies. So, instead of rejecting the numerical outcome from the EBA, we welcome it as a particular property of the Hénon attractor and, thus, as a provocative thought. In particular, we consider our result to support the conjectured non-self-similarity of the Hénon attractor. We would like to stress that we gained our intuition due to the EBA's ability to deal with negative q.

In this letter we have described a more efficient enlarged box algorithm (EBA) for estimating generalized dimensions. For deterministic self-similar measures, the EBA numerically renders an excellent agreement with the theoretical result in the whole range of values of q analysed, with small error bars and larger correlation coefficients. In analysing the Hénon attractor, we find dimensions for $q > 0$ which are in better agreement with some theoretical predictions than the numerical results from the SA. Using the EBA we estimate, for the first time with a fixed-size box-counting algorithm, the spectrum for large negative q, obtaining a very good performance and values also in good concordance with theory. We interpret the inflection shown by the spectrum as a numerical consequence of a 'phase transition' taking place between different multiplicative laws ruling the different regions of the attractor.

We thank Jordi Mach for many useful discussions and suggestions. RPS gratefully acknowledges a fellowship from the Museu de la Ciència de la Fundació 'la Caixa', Spain. RHR gratefully acknowledges partial support by a ONR grant N00014-90.J.1026.

References

[1] Mandelbrot B B 1982 *The Fractal Geometry of Nature* (San Francisco: Freeman)
[2] Witten T A and Sander L M 1981 *Phys. Rev. Lett.* **47** 1400
[3] Feder J 1988 *Fractals* (New York: Plenum)
[4] Schuster H G 1984 *Deterministic Chaos* (Weinheim: Physik)
[5] Mandelbrot B B 1974 *J. Fluid. Mech.* **62** 331
[6] Benzi R, Paladin G, Parisi G and Vulpiani A 1984 *J. Phys. A: Math. Gen.* **17** 3521
[7] Cawley R and Mauldin R D 1992 *Adv. Math.* **92** 196
[8] Falconer K J 1994 *J. Theor. Probability* **7** 681
[9] Riedi R H 1995 *J. Math. Anal. Appl.* **189** 462
[10] Halsey T, Jensen M, Kadanoff L, Procaccia I and Schraiman B 1986 *Phys. Rev.* A **33** 1141
[11] Grassberger P 1983 *Phys. Lett.* **97A** 227

[12] Hentschel H G E and Procaccia I 1983 *Physica* D **8** 435
[13] Grassberger P, Badii R and Politi A 1988 *J. Stat. Phys.* **51** 135
[14] Greenside H S, Wolf A, Swift J and Pignataro T 1982 *Phys. Rev.* A **25** 3453
[15] Giorgilli A, Casati D, Sironi L and Galgani L 1986 *Phys. Lett.* **115A** 202
[16] Liebovitch L S and Toth T 1989 *Phys. Lett.* **141A** 386
[17] Block A, von Bloh W and Schellnhuber H J 1990 *Phys. Rev.* A **42** 1869
[18] Hénon M 1976 *Commun. Math. Phys.* **50** 69
[19] Barnsley M 1988 *Fractals Everywhere* (New York: Academic)
[20] Mach J, Mas F and Sagués F 1995 *J. Phys. A: Math. Gen.* **28** 5607
[21] Arneodo A, Grasseau G and Kostelich E J 1987 *Phys. Lett.* **124A** 426
[22] Badii R and Broggi G 1988 *Phys. Lett.* **131A** 339
[23] Badii R and Politi A 1987 *Phys. Rev.* A **35** 1288
[24] Hata H, Morita T, Tomita K and Mori H 1987 *Prog. Theor. Phys.* **78** 721
[25] Lalley S P 1988 *Indiana Univ. Math. J.* **37** 699
[26] Radons G 1995 *Phys. Rev. Lett.* **75** 2518
[27] Riedi R H 1993 *PhD thesis* Zurich ETH